

On variational and symplectic time integrators for Hamiltonian systems

E. Gagarina^{a,*}, V.R. Ambati^a, S. Nurijanyan^a, J.J.W. van der Vegt^a,
O. Bokhove^{b,*}

^a Mathematics of Computational Science Group, Dept. of Applied Mathematics, University of Twente, P.O. Box 217, 7500 AE, Enschede, The Netherlands

^b School of Mathematics, University of Leeds, LS2 9JT, Leeds, United Kingdom

ARTICLE INFO

Article history:

Received 18 August 2015

Received in revised form 22 October 2015

Accepted 22 November 2015

Available online 2 December 2015

Keywords:

Nonlinear water waves

Finite element Galerkin method

(Non-)autonomous variational formulation

Symplectic time integration

ABSTRACT

Various systems in nature have a Hamiltonian structure and therefore accurate time integrators for those systems are of great practical use. In this paper, a finite element method will be explored to derive symplectic time stepping schemes for (non-)autonomous systems in a systematic way. The technique used is a variational discontinuous Galerkin finite element method in time. This approach provides a unified framework to derive known and new symplectic time integrators. An extended analysis for the new time integrators will be provided. The analysis shows that a novel third order time integrator presented in this paper has excellent dispersion properties. These new time stepping schemes are necessary to get accurate and stable simulations of (forced) water waves and other non-autonomous variational systems, which we illustrate in our numerical results.

© 2015 The Authors. Published by Elsevier Inc. This is an open access article under the CC BY license (<http://creativecommons.org/licenses/by/4.0/>).

1. Introduction

The dynamics of various physical phenomena, such as the movement of pendulums, planets, or water waves can be described in a variational framework. The development of variational principles for classical mechanics traces back to Euler, Lagrange, and Hamilton; an overview of this history can be found in [1,19]. This approach allows to express all the dynamics of a system in a single functional – the Lagrangian – which is an action integral. Hamiltonian mechanics is a reformulation of Lagrangian mechanics which provides a convenient framework to study the symmetry properties of a system. This is expressed by Noether's theorem which establishes the direct connection between the symmetry properties of Hamiltonian systems and conservation laws. When one approximates the system numerically, it is advantageous to preserve the Hamiltonian structure also at the discrete level. Given that Hamiltonian systems are abundant in nature, their numerical approximation is therefore a topic of significant relevance.

The topic of time integration of Hamiltonian systems has seen a rigorous development during the past decades. This has resulted in symplectic time integrators that have been designed to preserve the Hamiltonian structure for an approximated system. More information on symplectic integration of Hamiltonian systems can be found in [12] and [16]. According to the

* Corresponding authors.

E-mail addresses: E.Gagarina@utwente.nl (E. Gagarina), vrambati@gmail.com (V.R. Ambati), shavarsh.nurijanyan@utwente.nl (S. Nurijanyan), j.j.w.vandervegt@utwente.nl (J.J.W. van der Vegt), o.bokhove@leeds.ac.uk (O. Bokhove).

<http://dx.doi.org/10.1016/j.jcp.2015.11.049>

0021-9991/© 2015 The Authors. Published by Elsevier Inc. This is an open access article under the CC BY license (<http://creativecommons.org/licenses/by/4.0/>).

review in [20], variational time integrators can be proven to be symplectic by construction under certain conditions. In the variational approach, one can derive well-known schemes or new schemes, as reported in [10,17,22,26].

One of the most actively developed numerical methods is the finite element method with time discontinuous basis functions. Such a discontinuous Galerkin method in time was studied in [5–7]. In particular, the variational Galerkin finite element method in time was implemented in [11,20,22]. Integrators for variational principles including forcing were developed among others in [20].

The study of the variational time integrators that are discussed in this paper was motivated by our research into numerical discretizations of the equations describing nonlinear water waves, which have a Hamiltonian structure. The Hamiltonian structure of nonlinear gravity free surface water waves was shown by Zakharov [29]. In [9] (and [8]), we constructed a numerical water wave tank based on a discrete Miles' variational principle with forcing. The computational method had to fulfill a number of requirements in order to perform the simulations of the laboratory experiments presented in [14]. First, the experiments with which we compared numerical results run over a long period of time, covering also an extensive spatial domain, which meant that conservation of mass and bounded fluctuations of energy at the discrete level are important. Second, in one of the test cases in [9] (also [8]) a focussing wave was created with a wave height five times exceeding the ambient, incoming wave height. Therefore numerical stability had to be ensured. Third, a piston wave maker was used in the experiments, which gives external forcing to the system and results in a non-autonomous Hamiltonian system. It is non-trivial to meet all these requirements, in particular in combination with a spatial discretization of the nonlinear potential flow water wave equations. We therefore investigate variational time integrators in detail in that paper.

In the construction of variational time integrators we choose to work with a discontinuous Galerkin finite element method in time, because it allows additional freedom to develop new symplectic integrators, also for non-autonomous Hamiltonian systems. In this method the time domain is split into elements, and in each element the variables are approximated with polynomial expansions. The discrete variational principle is then obtained by substitution of the approximations in the continuum variational principle, provided one calculates the contributions of the delta functions that arise. After evaluation of the variational principle by calculating its variations, one obtains the discrete system of equations for the variational time integration method.

A crucial part of the discontinuous finite element method is the numerical flux arising from the before-mentioned delta functions. It has to be introduced to establish a connection between the time elements since in each element only a local polynomial approximation is used. We study a specially chosen numerical flux, somewhat inspired by the one explored in [24] and [25], which in turn was based on the theory of non-conservative products developed in [4] and [28]. The flux is also implemented in the numerical discretization for the nonlinear potential flow water wave equations, discussed in [8,9] and gives excellent results.

Combining the discrete variational principle with the derived numerical flux, we obtain a unified approach to construct time integrators for (non-)autonomous Hamiltonian systems. We have derived both well-known and novel symplectic time stepping schemes of first, second and third order accuracy. An extensive analysis for the discretizations is provided, including a linear stability analysis and an investigation of the symplectic nature of the schemes. The novel third order scheme we have developed is shown to have improved dispersion properties. Furthermore, within this approach we derive and test time stepping schemes for non-autonomous Hamiltonian systems, such as forced and damped oscillators. We study the approximation of forcing and damping terms considering the discrete versions of certain integrals.

In [10], a unified discontinuous Galerkin framework for time integration is given using weighted residuals for general nonlinear ordinary differential equations. New examples are given of two (implicit) symplectic Runge–Kutta methods, satisfying the symplectic condition by construction. Our work is complementary as we derive discrete variational principles by staying within the variational framework, which variation subsequently yields the nonlinear algebraic set of equations to be solved. While our schemes are always variational by construction, the symplectic and stability conditions need to be verified. These conditions can be met depending on the choice of quadrature we use and the choice of the free parameter(s) in the jump conditions. This complements Zhao and Wei's work [10], also because we developed our stable, variational and symplectic integrators for applications to water wave problems, since these can then be expressed as space and time discrete variational principles [9,27]. Extensions of the research presented here are found in Bokhove and Kalo-girou [3].

The outline of this paper is as follows. In Section 2 we introduce the dynamics of a Hamiltonian system with one degree of freedom. Next, Section 3 introduces the variational discontinuous Galerkin method. Here we obtain second order time stepping schemes, which can be formulated in the form of well-known symplectic schemes. In Section 4 a novel time integrator of third order accuracy in time is derived and analyzed. We analyze its linear stability and symplectic conditions. In Section 5 we present numerical results for non-autonomous systems by extending the well-known symplectic schemes we derived in this complementary variational framework. Our novel third order time integrator is used to simulate nonlinear water waves in Section 6. Conclusions are drawn in Sec. 7. More details on the analysis of the time integration methods are presented in two appendices.

2. Dynamics of a Hamiltonian system with one degree of freedom

The dynamics of a Hamiltonian system with one degree of freedom is embedded in the Lagrangian functional

$$\mathcal{L}(p, q) := \int_0^T \left(p \frac{dq}{dt} - H(p, q) \right) dt, \quad (1)$$

where $p(t)$ is the momentum, $q(t)$ the coordinate, and $H(p, q)$ the energy or Hamiltonian. The variational principle for the system is $\delta\mathcal{L} := \delta_p\mathcal{L} + \delta_q\mathcal{L} = 0$, where $\delta_p\mathcal{L}$ and $\delta_q\mathcal{L}$ are the functional derivatives with respect to p and q . The functional derivatives are defined as

$$\delta\mathcal{L} = \lim_{\epsilon \rightarrow 0} \frac{1}{\epsilon} (\mathcal{L}(p + \epsilon\delta p, q + \epsilon\delta q) - \mathcal{L}(p, q)). \quad (2)$$

Consider the variation of the Lagrangian functional (1)

$$\delta\mathcal{L}(p, q) = \int_0^T \left(\frac{dq}{dt} \delta p + p \frac{d\delta q}{dt} - \frac{\partial H}{\partial p} \delta p - \frac{\partial H}{\partial q} \delta q \right) dt = 0. \quad (3)$$

After integration by parts of (3), using the end point conditions $\delta q(0) = \delta q(T) = 0$, and the arbitrariness of the variations, the dynamics of a Hamiltonian system emerges as follows:

$$\delta p : \frac{dq}{dt} - \frac{\partial H}{\partial p} = 0 \quad \text{and} \quad \delta q : \frac{dp}{dt} + \frac{\partial H}{\partial q} = 0, \quad (4)$$

with initial conditions $p(t=0) = p_0$ and $q(t=0) = q_0$.

3. Variational discontinuous Galerkin time discretization of a Hamiltonian system

3.1. Discrete functional

The accurate numerical approximation of equations (4) is a well-developed subject of research. Geometric integrators target the preservation of system properties at the discrete level and symplectic integrators ensure that the approximated system is also Hamiltonian [12]. We start to approximate the Lagrangian (1) rather than approximating equations (4).

To approximate the functional (1) for a single-degree-of-freedom system in time, we first divide the time domain $[0, T]$ into N finite time intervals $I_n = (t_n, t_{n+1})$, $n = 0, \dots, N-1$, with length $\Delta t = t_{n+1} - t_n$. Each time interval I_n has a constant length and is related to a reference domain $\hat{I} = (-1, 1)$ through the mapping F_n , defined as

$$F_n : \hat{I} \rightarrow I_n : \tau \mapsto t = \frac{1}{2}(t_n(1 - \tau) + t_{n+1}(1 + \tau)). \quad (5)$$

Second, functions (p, q) are approximated element-wise with a polynomial expansion. In every element basis functions are continuous, but could be discontinuous across element boundaries. The finite element space is defined as

$$V^\tau := \{v^\tau \mid v^\tau \in L^2([0, T]), v^\tau|_{I_n} \in P_s(I_n), \forall I_n, n = 0, \dots, N-1\}, \quad (6)$$

where P_s is the space of polynomials of degree s . Each variable in finite element I_n is now approximated as $p^\tau \in V^\tau$, $q^\tau \in V^\tau$ and represented in a time slab (t_n, t_{n+1}) as

$$p^\tau = p^i \varphi^i, \quad q^\tau = q^i \psi^i, \quad (7)$$

with basis functions φ^i, ψ^i , which do not necessarily have to coincide, and expansion coefficients p^i, q^i . We will in particular consider Lagrange and Bernstein polynomials. Also, the Einstein summation convention will be used, which implies summation over repeating indices.

In order to account for the discontinuities at the element boundary we introduce the right and left traces of a variable $d(t)$ at time t_n as

$$d^{n,+} := \lim_{\epsilon \downarrow 0} d(t_n + \epsilon) \quad \text{and} \quad d^{n,-} := \lim_{\epsilon \downarrow 0} d(t_n - \epsilon), \quad (8)$$

respectively. At time level t_n the following jump $[[\cdot]]$ and average $\{\{\cdot\}\}_\alpha^\beta$ operators can then be defined

$$[[d]] \Big|_{t_n} = d^{n,-} - d^{n,+} \quad \text{and} \quad \{\{d\}\}_\alpha^\beta \Big|_{t_n} = \alpha d^{n,-} + \beta d^{n,+}, \quad (9)$$

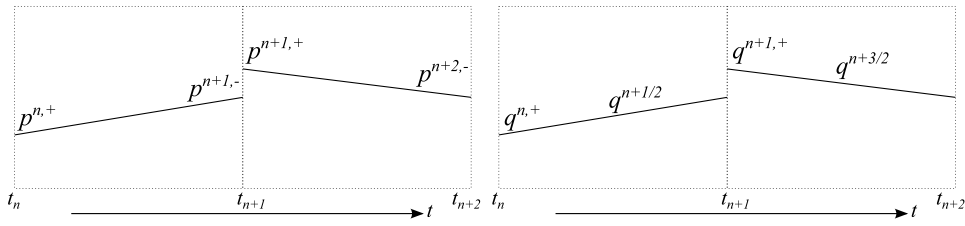


Fig. 1. Piecewise linear approximation in time.

where α, β are arbitrary real numbers with $\alpha + \beta = 1$ and $\alpha, \beta \geq 0$. The discrete functional for the Hamiltonian system (1) is now obtained after introducing polynomial approximations of p and q into the functional and splitting of the time integral into a summation over time intervals

$$\mathcal{L}^\tau(p^\tau, q^\tau) := \sum_{n=0}^{N-1} \int_{t_n}^{t_{n+1}} \left(p^\tau \frac{dq^\tau}{dt} - H(p^\tau, q^\tau) \right) dt - \sum_{n=-1}^{N-1} [[q^\tau]] \{ \{ p^\tau \} \}_\alpha^\beta \Big|_{t_{n+1}}. \tag{10}$$

The last term in (10) comes as a numerical flux.¹ The flux is required to establish a connection between the time element boundaries, as we use discontinuous basis functions.

There is still some freedom in the definition of the discrete Lagrangian (10). In the first place we need to specify the polynomial order of the basis functions. As in general it is not possible or desirable to compute the integral of the Hamiltonian analytically, we also have to choose a quadrature rule [20]. In [13] it is proven that the order of the quadrature rule will give an upper bound for the attainable order of the time integration scheme. Finally, the choice of the weight α in the flux term also leaves some freedom to derive and optimize different time integration methods.

The derivation of a time integration scheme is now performed as follows. We choose a polynomial approximation of order s . To obtain a scheme of order $s + 1$ we should take a quadrature rule with an order of accuracy that is at least $s + 1$ [13]. After the scheme is derived, a linear stability analysis will be performed to find appropriate weights α in the flux term. For our novel scheme further analysis is done to show that the scheme is symplectic.

3.2. Second order variational time discretization: Störmer–Verlet

We have rederived and reinterpreted the symplectic Euler scheme as a genuine discontinuous Galerkin scheme with piecewise constant polynomials for p and q , in each time slab, as well as the (modified) midpoint scheme using a discontinuous Galerkin scheme in which p and q are expanded using quadratic polynomials and both evaluated at the mid-points $p^{n+1/2}$ and $q^{n+1/2}$ of the integration interval only (see, [8]).

Next we show how this can be done for a scheme of second order accuracy because we use an extension of the resulting Störmer–Verlet scheme for the non-autonomous systems considered in §5. To obtain a second order time integrator we need to choose linear basis functions in the polynomial expansions. Various options for the approximation of the variables and integrals are possible. Since we want to derive the known Störmer–Verlet scheme in our new approach, we take the trapezoidal rule for p and the midpoint rule for q , yielding

$$\int_{t_n}^{t_{n+1}} H(p^\tau, q^\tau) dt = \frac{\Delta t}{2} \left(H(p^{n,+}, q^{n+1/2}) + H(p^{n+1,-}, q^{n+1/2}) \right), \tag{11}$$

where the expansion coefficient $q^{n+1/2}$ is the value in the middle of the time interval. We approximate the variables in each time element I_n as

$$p^\tau = \frac{t^{n+1} - t}{\Delta t} p^{n,+} + \frac{t - t^n}{\Delta t} p^{n+1,-}, \tag{12a}$$

$$q^\tau = \frac{2(t - t^n)}{\Delta t} q^{n+1/2} + \frac{t^n + t^{n+1} - 2t}{\Delta t} q^{n,+}, \tag{12b}$$

see Fig. 1. Introducing (11)–(12) in the discrete functional (10), we obtain

¹ For alternative derivations and further background on this type of numerical flux, see Appendix C in [9] and [3,24,25].

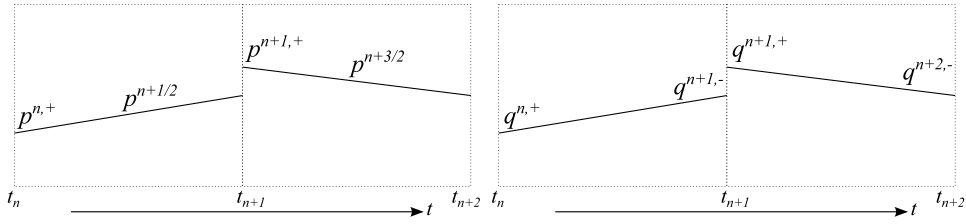


Fig. 2. Piecewise linear approximation in time.

$$\mathcal{L}^\tau(p^\tau, q^\tau, t) = \sum_{n=0}^{N-1} \left((p^{n,+} + p^{n+1,-})(q^{n+1/2} - q^{n,+}) - \frac{\Delta t}{2} (H(p^{n,+}, q^{n+1/2}) + H(p^{n+1,-}, q^{n+1/2})) \right) - \sum_{n=-1}^{N-1} (2q^{n+1/2} - q^{n,+} - q^{n+1,+})(\alpha p^{n+1,-} + \beta p^{n+1,+}). \tag{13}$$

Applying the variational principle $\delta\mathcal{L}^\tau = 0$, using the arbitrariness of the variations and end-point conditions $\delta(2q^{-1/2} - q^{-1,+}) := \delta q^{0,-} = 0, \delta p^{0,-} = 0, \delta q^{N,+} = 0, \delta p^{N,+} = 0$, we obtain the following variational time integrator

$$\delta q^{n,+} : (\beta - 1)p^{n,+} + (\alpha - 1)p^{n+1,-} + \beta p^{n+1,+} + \alpha p^{n,-} = 0, \tag{14a}$$

$$\delta p^{n,+} : q^{n+1/2} = q^{n,+} + \beta(2q^{n-1/2} - q^{n-1,+} - q^{n,+}) + \frac{\Delta t}{2} \frac{\partial H(p^{n,+}, q^{n+1/2})}{\partial p^{n,+}}, \tag{14b}$$

$$\delta q^{n+1/2} : 2\beta p^{n+1,+} + (2\alpha - 1)p^{n+1,-} = p^{n,+} - \frac{\Delta t}{2} \left(\frac{\partial H(p^{n,+}, q^{n+1/2})}{\partial q^{n+1/2}} + \frac{\partial H(p^{n+1,-}, q^{n+1/2})}{\partial q^{n+1/2}} \right), \tag{14c}$$

$$\delta p^{n+1,-} : q^{n+1/2} - \alpha(2q^{n+1/2} - q^{n,+} - q^{n+1,+}) = q^{n,+} + \frac{\Delta t}{2} \frac{\partial H(p^{n+1,-}, q^{n+1/2})}{\partial p^{n+1,-}}. \tag{14d}$$

In Appendix B we show that this scheme is stable for weights $\alpha \in [0.5, 1]$ and coincides under this choice with the well-known second order Störmer-Verlet time integrator. It is interesting to note that we start with two discontinuous variables, but at the end there is no jump in p at the time levels $t_n, n = 0, \dots, N$ anymore. Moreover, the presence of a jump in the q variable does not result in a scheme different from the classical one (see Appendix B).

An adjoint Störmer-Verlet scheme can be obtained via a swapped linear approximation of the variables in each element I_n

$$q^\tau = \frac{t^{n+1} - t}{\Delta t} q^{n,+} + \frac{t - t^n}{\Delta t} q^{n+1,-}, \tag{15a}$$

$$p^\tau = \frac{2(t - t^n)}{\Delta t} p^{n+1/2} + \frac{t^n + t^{n+1} - 2t}{\Delta t} p^{n,+}, \tag{15b}$$

see Fig. 2, and a trapezoidal rule for q and a midpoint rule for p

$$\int_{t_n}^{t_{n+1}} H(p^\tau, q^\tau) dt = \frac{\Delta t}{2} (H(p^{n+1/2}, q^{n,+}) + H(p^{n+1/2}, q^{n+1,-})). \tag{16}$$

Analogously to the previous case, it can be shown that this weighted scheme is stable for $\alpha \in [0, 0.5]$ and a reformulation allows to recover a well known formulation of the scheme, as given in [12].

4. New variational time integrators

A natural question is whether it is possible to find new time integrators following the variational approach described in the previous section. In this section we will construct a new time integration scheme with third order accuracy using the variational approach. We will investigate convergence, symplecticity, linear stability and dispersion properties.

4.1. Third order scheme

To obtain a third order scheme we choose in each time element I_n the following quadratic Lagrange basis functions

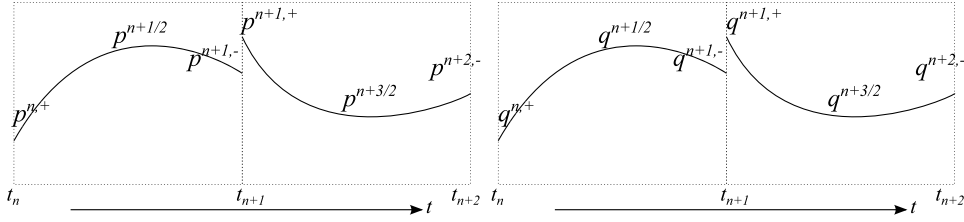


Fig. 3. Piecewise quadratic approximation in time.

$$p^\tau = \frac{(t^n + t^{n+1} - 2t)(t^{n+1} - t)}{\Delta t^2} p^{n,+} + \frac{4(t - t^n)(t^{n+1} - t)}{\Delta t^2} p^{n+1/2} - \frac{(t^n + t^{n+1} - 2t)(t - t^n)}{\Delta t^2} p^{n+1,-}, \tag{17a}$$

$$q^\tau = \frac{(t^n + t^{n+1} - 2t)(t^{n+1} - t)}{\Delta t^2} q^{n,+} + \frac{4(t - t^n)(t^{n+1} - t)}{\Delta t^2} q^{n+1/2} - \frac{(t^n + t^{n+1} - 2t)(t - t^n)}{\Delta t^2} q^{n+1,-}, \tag{17b}$$

as can be seen in Fig. 3. There are three independent expansion coefficients present in the polynomial representation: $p^{n,+}$ at the left boundary of the interval, $p^{n+1/2}$ at the middle of the interval and $p^{n+1,-}$ at the right boundary of the interval and similarly for q . We approximate the integral over the Hamiltonian with Simpson's third order quadrature rule as

$$\int_{t_n}^{t_{n+1}} H(p^\tau, q^\tau) dt \cong \frac{\Delta t}{6} (H(p^{n,+}, q^{n,+}) + 4H(p^{n+1/2}, q^{n+1/2}) + H(p^{n+1,-}, q^{n+1,-})). \tag{18}$$

The discrete functional (10) then becomes

$$\begin{aligned} \mathcal{L}^\tau(p^\tau, q^\tau) = & \sum_{n=0}^{N-1} \int_{t^n}^{t^{n+1}} p^\tau \frac{dq^\tau}{dt} dt - \frac{\Delta t}{6} (H(p^{n,+}, q^{n,+}) + 4H(p^{n+1/2}, q^{n+1/2}) + H(p^{n+1,-}, q^{n+1,-})) \\ & - \sum_{n=-1}^{N-1} (q^{n+1,-} - q^{n+1,+})(\alpha p^{n+1,-} + \beta p^{n+1,+}). \end{aligned} \tag{19}$$

This choice of quadrature rule and basis functions corresponds to the choices made in [22] for the scheme called "P2N3Q4Lob" in their paper (keeping this acronym). Nevertheless, the resulting scheme is different due to the choice of the numerical flux.

Applying the variational principle $\delta \mathcal{L}^\tau = 0$, using the arbitrariness of the variations and end-point conditions $\delta q^{0,-} = 0$, $\delta p^{0,-} = 0$, $\delta q^{N,+} = 0$, $\delta p^{N,+} = 0$, we get a new third order scheme

$$q^{n+1/2} = (1 - \frac{3}{2}\beta)q^{n,+} + \frac{3}{2}\beta q^{n,-} + \frac{\Delta t}{4} \left(\frac{\partial H(p^{n,+}, q^{n,+})}{\partial p^{n,+}} + \frac{\partial H(p^{n+1/2}, q^{n+1/2})}{\partial p^{n+1/2}} \right), \tag{20a}$$

$$p^{n+1/2} = (1 - \frac{3}{2}\alpha)p^{n,+} + \frac{3}{2}\alpha p^{n,-} - \frac{\Delta t}{4} \left(\frac{\partial H(p^{n,+}, q^{n,+})}{\partial q^{n,+}} + \frac{\partial H(p^{n+1/2}, q^{n+1/2})}{\partial q^{n+1/2}} \right), \tag{20b}$$

$$q^{n+1,-} = q^{n,+} + \Delta t \frac{\partial H(p^{n+1/2}, q^{n+1/2})}{\partial p^{n+1/2}}, \tag{20c}$$

$$p^{n+1,-} = p^{n,+} - \Delta t \frac{\partial H(p^{n+1/2}, q^{n+1/2})}{\partial q^{n+1/2}}, \tag{20d}$$

$$\alpha q^{n+1,+} = -\frac{1}{6}q^{n,+} + \frac{2}{3}q^{n+1/2} + (\alpha - \frac{1}{2})q^{n+1,-} + \frac{\Delta t}{6} \frac{\partial H(p^{n+1,-}, q^{n+1,-})}{\partial p^{n+1,-}}, \tag{20e}$$

$$\beta p^{n+1,+} = -\frac{1}{6}p^{n,+} + \frac{2}{3}p^{n+1/2} + (\beta - \frac{1}{2})p^{n+1,-} - \frac{\Delta t}{6} \frac{\partial H(p^{n+1,-}, q^{n+1,-})}{\partial q^{n+1,-}}. \tag{20f}$$

Equations (20a) and (20b) have to be solved together as an implicit system. The other four equations are explicit.

4.1.1. Linear stability

To perform the linear stability analysis we introduce the Hamiltonian of the harmonic oscillator $H(p, q) = \frac{1}{2}\omega^2 q^2 + \frac{1}{2}p^2$ into scheme (20). With the prescribed Hamiltonian we can formulate scheme (20) in a form

$$(p^{n+1,-}, q^{n+1,-}, p^{n+1,+}, q^{n+1,+})^T = A(p^{n,-}, q^{n,-}, p^{n,+}, q^{n,+})^T. \tag{21}$$

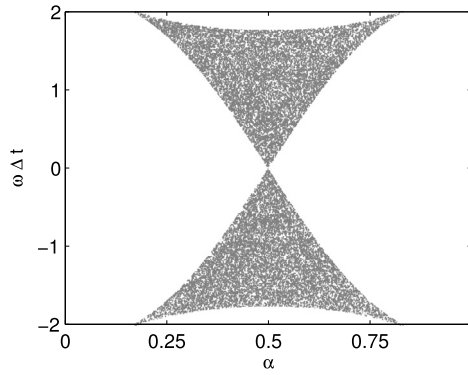


Fig. 4. Modulus of eigenvalues λ_i of system (20) for a linear harmonic oscillator. The shadowed area corresponds to the region where the modulus of all the eigenvalues is equal to one, i.e., where the scheme is stable.

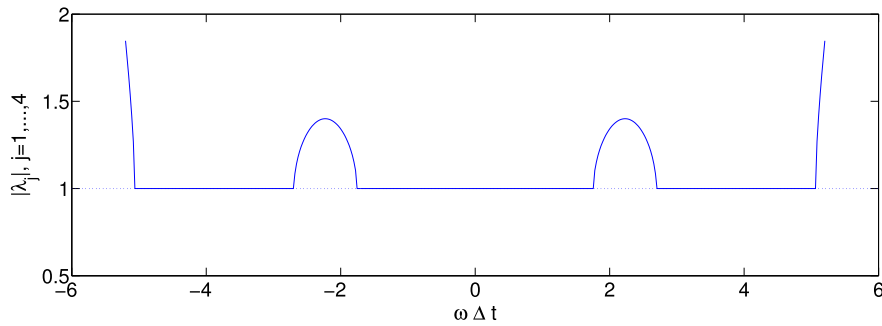


Fig. 5. Modulus of the eigenvalues for the linear system (22) with $\alpha = 0.5$ – solid line versus $\lambda = 1$ – dotted line.

To ensure that the numerical solution is bounded, it is required for the eigenvalues λ_i of the matrix A to be less than or equal to one in modulus [12]. The characteristic polynomial of the matrix A is a quartic function in λ . Since, the explicit form of the eigenvalues is complicated we therefore compute the stability criteria numerically in Matlab. We take a range of weights α , a range of frequencies multiplied by time step $\omega\Delta t$, substitute them into the expressions for the exact solutions of a quartic function, and show the domains where the maximum in modulus eigenvalue is smaller than one $\max_{i=1,\dots,4} |\lambda_i| \leq 1$. One can see in Fig. 4 that the only stability region located near $\omega\Delta t = 0$ is the one corresponding to $\alpha = 0.5$.

For $\alpha = 0.5$ and the Hamiltonian of the harmonic oscillator the transformation matrix becomes equal to

$$A = \begin{pmatrix} -\frac{3}{5}g & -\frac{12g}{5\Delta t} & 1-g & -\omega^2\Delta t\frac{1-g}{4} \\ \frac{12g}{5\Delta t\omega^2} & -\frac{3}{5}g & \Delta t\frac{1-g}{4} & 1-g \\ 1-g & -\omega^2\Delta t\frac{1-g}{4} & \frac{1}{15}g(\Delta t^2\omega^2-9) & \frac{4g}{15\Delta t}(\Delta t^2\omega^2-9) \\ \Delta t\frac{1-g}{4} & 1-g & -\frac{4g}{15\Delta t\omega^2}(\Delta t^2\omega^2-9) & \frac{1}{15}g(\Delta t^2\omega^2-9) \end{pmatrix}, \tag{22}$$

where $g = \frac{5\Delta t^2\omega^2}{\Delta t^2\omega^2+16}$. The eigenvalues are computed numerically, see Fig. 5, which is a two-dimensional slice of the plot in Fig. 4 with a fixed weight $\alpha = 0.5$. Within the (grey) stability domain, all the eigenvalues are equal to one in modulus, which leads to an absence of dissipation in the numerical scheme. The numerical calculation of the eigenvalues provides the linear stability condition $|\omega\Delta t| \leq 1.757$, which is slightly more restrictive than the criteria for the Störmer–Verlet scheme. Compared with the scheme *P2N3Q4Lob* in [22], we see that bumps are present in the linear stability domain for both cases, but the stability restriction for *P2N3Q4Lob* is less restrictive and equals $|\omega\Delta t| \leq 2\sqrt{2}$. As the authors mention in [22], the scheme *P2N3Q4Lob* is implicit and all the equations have to be solved simultaneously, which may pose a more difficult numerical challenge. The third order scheme proposed here does not possess this shortcoming, as will be demonstrated further.

Since the value $\alpha = 0.5$ gives the best stability results, the time integration scheme (20) becomes

$$q^{n+1/2} = \frac{3}{4}q^{n,-} + \frac{1}{4}q^{n,+} + \frac{\Delta t}{4} \left(\frac{\partial H(p^{n,+}, q^{n,+})}{\partial p^{n,+}} + \frac{\partial H(p^{n+1/2}, q^{n+1/2})}{\partial p^{n+1/2}} \right), \tag{23a}$$

$$p^{n+1/2} = \frac{3}{4}p^{n,-} + \frac{1}{4}p^{n,+} - \frac{\Delta t}{4} \left(\frac{\partial H(p^{n,+}, q^{n,+})}{\partial q^{n,+}} + \frac{\partial H(p^{n+1/2}, q^{n+1/2})}{\partial q^{n+1/2}} \right), \tag{23b}$$

Table 1

Convergence in L^∞ -, L^2 -norms of the error in q for a harmonic oscillator, and L^∞ -error in the energy of the system. Initial conditions are $q^{0,-} = q^{0,+} = -0.001$, $p^{0,-} = p^{0,+} = 0$, $\omega^2 = 0.1$, the biggest time step $\Delta t = 1$, the final time $T = 40$. The precision set to solve the implicit system is $\epsilon = 10^{-12}$.

Step	q		q		Energy	
	L^∞ -error	order	L^2 -error	order	ΔH -error	order
Δt	4.1204E-6	–	6.1191E-6	–	1.3489E-9	–
$\Delta t/2$	5.1937E-7	2.9879	7.0457E-7	3.1185	1.6565E-10	3.0256
$\Delta t/4$	6.5058E-8	2.9970	8.6159E-8	3.0317	2.0613E-11	3.0065
$\Delta t/8$	8.1366E-9	2.9992	1.0710E-8	3.0081	2.5735E-12	3.0017
$\Delta t/16$	1.0172E-9	2.9998	1.3369E-9	3.0020	3.2171E-13	2.9999
$\Delta t/32$	1.2716E-10	3.0000	1.6705E-10	3.0005	4.0211E-14	3.0001
$\Delta t/64$	1.5895E-11	3.0000	2.0879E-11	3.0001	5.0263E-15	3.0000

$$q^{n+1,-} = q^{n,+} + \Delta t \frac{\partial H(p^{n+1/2}, q^{n+1/2})}{\partial p^{n+1/2}}, \tag{23c}$$

$$p^{n+1,-} = p^{n,+} - \Delta t \frac{\partial H(p^{n+1/2}, q^{n+1/2})}{\partial q^{n+1/2}}, \tag{23d}$$

$$q^{n+1,+} = \frac{4}{3}q^{n+1/2} - \frac{1}{3}q^{n,+} + \frac{\Delta t}{3} \frac{\partial H(p^{n+1,-}, q^{n+1,-})}{\partial p^{n+1,-}}, \tag{23e}$$

$$p^{n+1,+} = \frac{4}{3}p^{n+1/2} - \frac{1}{3}p^{n,+} - \frac{\Delta t}{3} \frac{\partial H(p^{n+1,-}, q^{n+1,-})}{\partial q^{n+1,-}}. \tag{23f}$$

The accuracy of the scheme (23) is verified for a linear system with Hamiltonian $H = \frac{1}{2}p^2 + \frac{1}{2}\omega^2q^2$. The results in Table 1 show that the scheme (23) is third order accurate. We define the L^2 error as $L^2_{err} = \sqrt{\sum_{n=1}^N \int_{t^{n-1}}^{t^n} (q^\tau - q_{ex}(t))^2 dt}$ for the polynomial approximation q^τ defined in (17b) and the exact solution q_{ex} of the autonomous system derived in (A.8). The final results of the scheme are the values $q^{n+1,+}$, $p^{n+1,+}$; therefore the L^∞ -error and ΔH -error are defined as

$$L^\infty_{err} = \max_{1 \leq n \leq N} |q^{n,+} - q_{ex}(t^n)|, \tag{24a}$$

$$\Delta H_{err} = \max_{1 \leq n \leq N} (H(p^{n,+}, q^{n,+})) - \min_{1 \leq n \leq N} (H(p^{n,+}, q^{n,+})). \tag{24b}$$

4.1.2. Dispersion relation

The dispersion analysis is performed following [15]. In order to compute the dispersion properties of the new variational time integration scheme (23), we take the Fourier modes (i.e., we now take $\lambda = e^{-i\hat{\omega}\Delta t}$ such that $|\lambda| = 1$)

$$\begin{pmatrix} p^{n,-} \\ q^{n,-} \\ p^{n,+} \\ q^{n,+} \end{pmatrix} = \begin{pmatrix} ae^{-i\hat{\omega}n\Delta t} \\ be^{-i\hat{\omega}n\Delta t} \\ ce^{-i\hat{\omega}n\Delta t} \\ de^{-i\hat{\omega}n\Delta t} \end{pmatrix} \tag{25}$$

and substitute these into the system (23), which gives a linear system

$$e^{-i\hat{\omega}\Delta t}(a, b, c, d)^T = A(a, b, c, d)^T. \tag{26}$$

In general, we are not interested in the results for the variables $p^{n+1,-}$, $q^{n+1,-}$, as those are intermediate data. What matters is a relation for the variables $p^{n+1,+}$, $q^{n+1,+}$. In the continuum case, as shown in Appendix A, the exact dispersion relation is $c = \pm id\omega$, cf. (A.7). Nevertheless, as there are four equations, all of them have to be included in the analysis. We manipulate system of equations (26) symbolically with Matlab to find the relations between a , b , c and d ; and, to obtain the numerical frequency $\hat{\omega}$.

For the dispersion analysis we introduce the variables

$$x = \sqrt{1 - \frac{\Delta t^6 \omega^6}{36(4 - \Delta t^2 \omega^2)^2}}, \quad y = \frac{\Delta t^3 \omega^3}{6(4 - \Delta t^2 \omega^2)}. \tag{27}$$

Notice, that $x \rightarrow 1$, $y \rightarrow 0$, when $\Delta t \rightarrow 0$. The first family of solutions of (26) is

$$a = -ib\omega, \quad c = -id\omega, \quad b = -(x + iy)d, \tag{28a}$$

$$\hat{\omega} = \frac{1}{\Delta t} \arccos \frac{-4(4 - \Delta t^2 \omega^2)x + \Delta t^2 \omega^2 (\frac{\Delta t^2 \omega^2}{6} - 3)}{\Delta t^2 \omega^2 + 16}. \tag{28b}$$

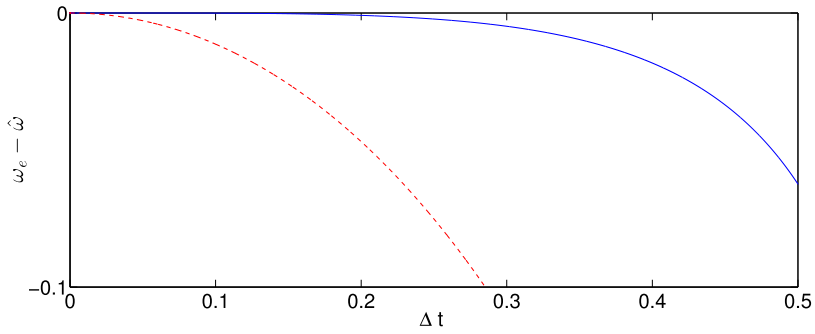


Fig. 6. A difference between numerical and exact frequencies $\omega - \hat{\omega}$. The red dash line presents the dispersion relation for the Störmer–Verlet scheme and the blue solid line the dispersion relation (29b) for the third order scheme (23).

We see, that the second relation in (28) is the exact one. The numerical frequency is, however, wrong as can be verified by taking the limit $\Delta t \rightarrow 0$ in (28b).

The second family of solutions is

$$a = -ib\omega, \quad c = -id\omega, \quad b = (x - iy)d, \tag{29a}$$

$$\hat{\omega} = \frac{1}{\Delta t} \arccos \frac{4(4 - \Delta t^2 \omega^2)x + \Delta t^2 \omega^2 (\frac{\Delta t^2 \omega^2}{6} - 3)}{\Delta t^2 \omega^2 + 16}. \tag{29b}$$

The relation $c = -id\omega$ is the exact dispersion relation, and the numerical frequency converges to the exact one $\hat{\omega} \rightarrow \omega$ if $\Delta t \rightarrow 0$ in (29b), see Fig. 6.

The third family of solutions is

$$a = ib\omega, \quad c = id\omega, \quad b = (x + iy)d, \tag{30a}$$

$$\hat{\omega} = -\frac{1}{\Delta t} \arccos \frac{4(4 - \Delta t^2 \omega^2)x + \Delta t^2 \omega^2 (\frac{\Delta t^2 \omega^2}{6} - 3)}{\Delta t^2 \omega^2 + 16}. \tag{30b}$$

In this case the numerical frequency converges to the negative value, $\hat{\omega} \rightarrow -\omega$ when $\Delta t \rightarrow 0$.

The fourth family of solutions is

$$a = ib\omega, \quad c = id\omega, \quad b = (-x + iy)d, \tag{31a}$$

$$\hat{\omega} = -\frac{1}{\Delta t} \arccos \frac{-4(4 - \Delta t^2 \omega^2)x + \Delta t^2 \omega^2 (\frac{\Delta t^2 \omega^2}{6} - 3)}{\Delta t^2 \omega^2 + 16}. \tag{31b}$$

Here the numerical frequency does not converge to the correct value when $\Delta t \rightarrow 0$.

Since there are two parasitic modes we need to be careful that they do not pollute the solution. For the parasitic modes the relation $b \rightarrow -d$ holds. One important step is to choose $a = c$ and $b = d$, i.e. take $p^{0,-} = p^{0,+}$ and $q^{0,-} = q^{0,+}$ as initial conditions. In this case the parasitic modes are eliminated. For the nonlinear water wave case we verified the consequence of this initial filtering numerically in §6, which appears to be sufficient to ensure stability in the nonlinear case. This absence of an initial jump leads to satisfactory results.

4.1.3. Symplecticity

If a one-degree-of-freedom Hamiltonian system is approximated with two variables p^n and q^n , the symplecticity condition is formulated as

$$M^T J^{-1} M = J^{-1}, \tag{32}$$

where the Jacobian of the transformation is defined as

$$M = \frac{\partial(q^{n+1}, p^{n+1})}{\partial(q^n, p^n)}. \tag{33}$$

The structure matrix J , equal to

$$J = \begin{pmatrix} 0 & I \\ -I & 0 \end{pmatrix}, \tag{34}$$

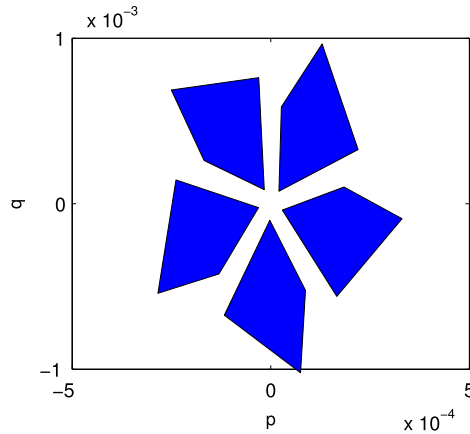


Fig. 7. Evolution of variables $(p^{n,+}, q^{n,+})$ in phase space over one time period. System (23) with $\omega = 0.3162$, $\Delta t = 0.2484$ is solved for four initial conditions. The error in solving the linear system in the implicit step of (23) is set to $\epsilon = 10^{-15}$.

where I is the identity matrix with the dimension equal to the degrees of freedom of the Hamiltonian system, relates to the Hamiltonian system as

$$\begin{pmatrix} q \\ p \end{pmatrix}_t = J \nabla H = \begin{pmatrix} 0 & 1 \\ -1 & 0 \end{pmatrix} \begin{pmatrix} H_q \\ H_p \end{pmatrix}. \tag{35}$$

Here the subscript $(\cdot)_t$ refers to taking a time derivative and $H_q \equiv \partial H / \partial q$, etc. For details we refer to [12]. Since we are working with an extended system, i.e. a one-degree-of-freedom Hamiltonian system is approximated with four variables $p^{n,-}, p^{n,+}$ and $q^{n,-}, q^{n,+}$, the matrices in the symplecticity condition (32) are also extended. We take

$$M = \frac{\partial(q^{n+1,-}, q^{n+1,+}, p^{n+1,-}, p^{n+1,+})}{\partial(q^{n,-}, q^{n,+}, p^{n,-}, p^{n,+})}, \tag{36}$$

and the structure matrix J , defined as in (34) for a two-dimensional system. The Hamiltonian system can then be written as

$$\begin{pmatrix} q^- \\ q^+ \\ p^- \\ p^+ \end{pmatrix}_t = (J) \nabla H = \begin{pmatrix} 0 & 0 & 0 & 1 \\ 0 & 0 & 1 & 0 \\ 0 & -1 & 0 & 0 \\ -1 & 0 & 0 & 0 \end{pmatrix} \begin{pmatrix} H_{q^-} \\ H_{q^+} \\ H_{p^-} \\ H_{p^+} \end{pmatrix}. \tag{37}$$

We verified in Matlab using symbolic manipulation that the condition (32) is valid for the new system (23). The details of the matrix M are not given explicitly here since the expressions are too large to present.

For a Hamiltonian system with one degree of freedom the symplecticity condition means preservation of an area in phase space [12]. A phase-space plane is shown in Fig. 7. A point on the plane is given as $(p^{n,+}, q^{n,+})$, as our prime interest lies in these variables. We define four initial conditions in the plane, that constitute a quadrilateral shape. The numerical approximation of a harmonic oscillator system develops according to the scheme (23). The system cycles over time through the same states, which are defined by the initial conditions. The area of the rectangular shape oscillates around the initial state, see Fig. 8.

From a geometrical point of view, the symplecticity condition (32) means in the general case with $d > 1$ degrees of freedom that the sum of the oriented areas of the projections of a shape in $2d$ space onto the planes (p^i, q^i) is conserved [12]. Therefore Figs. 7 and 8 do not prove symplecticity, but illustrate the property of the plus-variables $p^{n,+}, q^{n,+}$ to cycle through the same states.

The conclusions on the novel third order scheme (23) are as follows. The scheme is symplectic, but the linear stability condition is more restrictive than the condition for the Störmer–Verlet scheme. The scheme is third order accurate, which is verified both for linear and nonlinear problems (see §6 and also Bokhove and Kalogirou [3]).

5. Applications to non-autonomous systems

In the following section, we develop time integration of non-autonomous Hamiltonian systems.

5.1. Damped oscillator

Consider a damped one-degree-of-freedom Hamiltonian system with the following non-autonomous variational principle, (see [23] and [27] for related examples):

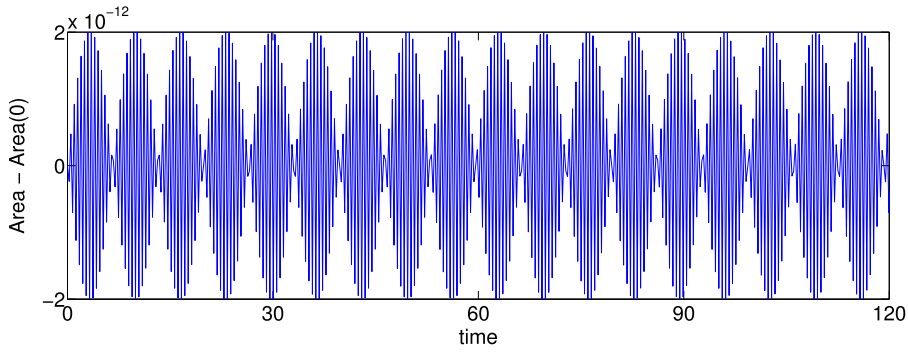


Fig. 8. Oscillation in the area of a quadrilateral shape in phase-space shown in Fig. 7 for the harmonic oscillator computed with the third order accurate symplectic time integrator (23). System (23) is solved over 10 time periods with $\omega = 0.3162$, $\Delta t = 0.2484$. The precision in solving the implicit step in (23) is set to $\epsilon = 10^{-15}$.

$$\begin{aligned}
 0 &= \delta \tilde{\mathcal{L}}(p, q) = \delta \int_0^T \left(p \frac{dq}{dt} - H(p, q) \right) e^{\gamma t} dt \\
 &= \int_0^T \left(\frac{dq}{dt} - \frac{\partial H}{\partial p} \right) \delta(p e^{\gamma t}) - \left(\frac{d(p e^{\gamma t})}{dt} + \frac{\partial H}{\partial q} e^{\gamma t} \right) \delta q dt + p e^{\gamma t} \delta q \Big|_0^T,
 \end{aligned} \tag{38}$$

with $\gamma > 0$ the coefficient of the linear momentum damping and end-point conditions $\delta q(0) = \delta q(T) = 0$. Variation of (38) with respect to the variables p and q yields Hamilton’s equations for the damped oscillator when the Hamiltonian is $H(p, q) = \frac{1}{2}p^2 + \frac{1}{2}q^2$ (and unit frequency). We find

$$\delta(p e^{\gamma t}) : \quad \frac{dq}{dt} = \frac{\partial H}{\partial p} = p, \tag{39a}$$

$$\delta q : \quad \frac{dp}{dt} + \gamma p = -\frac{\partial H}{\partial q} = -q. \tag{39b}$$

With the coordinate transformation $q = Q \exp(-\gamma t/2)$ and $p = P \exp(-\gamma t/2)$, the variational principle then becomes

$$0 = \delta \int_0^T \left(P \frac{dQ}{dt} - \tilde{H}(P, Q) \right) dt, \tag{40}$$

with modified Hamiltonian

$$\tilde{H}(P, Q) = \frac{1}{2}P^2 + \frac{1}{2}Q^2 + \frac{1}{2}\gamma P Q. \tag{41}$$

Hence, the system (40) is reformulated as an autonomous system, viz. the modified Hamiltonian (41) is time independent in the new variables P and Q . We can now monitor this modified Hamiltonian at the discrete level.

5.1.1. Discretization

We start with a first order approximation of the functional (38) in time. We consider the discrete variational principle

$$\tilde{\mathcal{L}}^\tau(p^\tau, q^\tau) := \sum_{n=0}^{N-1} \int_{t^n}^{t^{n+1}} \left(p^\tau \frac{dq^\tau}{dt} - H(p^\tau, q^\tau) \right) e^{\gamma t} dt - \sum_{n=-1}^{N-1} \left[[q^\tau] \right] \left\{ p^\tau e^{\gamma t} \right\} \Big|_{t_{n+1}}^\beta, \tag{42}$$

where the variables (p, q) are approximated as piecewise-constant per time interval (t^n, t^{n+1}) . As in [8], to obtain the well-known formulation of the symplectic Euler scheme, we rename the approximations as $q^\tau = q^{n,+}$, $p^\tau = p^{n+1,-}$ and take $\alpha = 1$, $\beta = 0$. The exponential time-dependent term responsible for the damping is new and will be approximated using the value at the right boundary of the time element $e^{\gamma t^{n+1}}$.

Substituting these approximations into (42), we obtain

$$\tilde{\mathcal{L}}^\tau(p^\tau, q^\tau) := \sum_{n=0}^{N-1} -\Delta t H(p^{n+1,-}, q^{n,+}) e^{\gamma t^{n+1}} - \sum_{n=-1}^{N-1} (q^{n,+} - q^{n+1,+}) (p^{n+1,-} e^{\gamma t^{n+1}}). \tag{43}$$

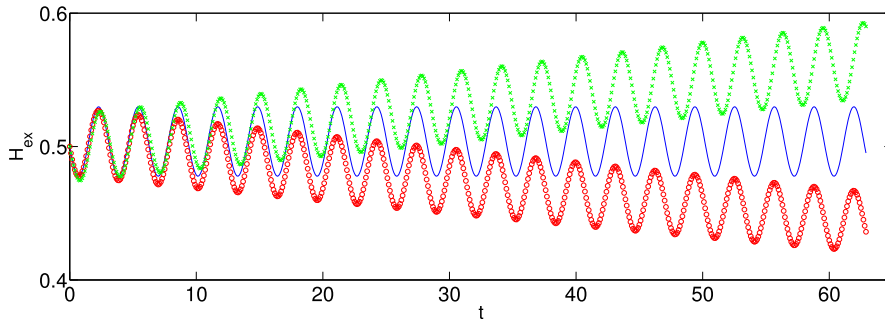


Fig. 9. Modified total energy H_{ex} for a damped oscillator versus time. The discrete modified energy for approximation (44a) is plotted as a solid line, the discrete modified energy for approximation (48) is plotted with crosses and the discrete modified energy for approximation (47) is plotted versus time with circles.

We take variations $\delta\tilde{\mathcal{L}}^\tau = 0$ of (43) with respect to the variables $p^{n+1,-}$, $q^{n,+}$, use the arbitrariness of variations and end-point conditions $\delta q^{0,-} = 0$, $\delta p^{0,-} = 0$, $\delta q^{N,+} = 0$, to obtain

$$p^{n+1,-} = p^{n,-} - \Delta t \frac{\partial H(p^{n+1,-}, q^{n,+})}{\partial q^{n,+}} - (1 - e^{\gamma(t^n - t^{n+1})})p^{n,-}, \tag{44a}$$

$$q^{n+1,+} = q^{n,+} + \Delta t \frac{\partial H(p^{n+1,-}, q^{n,+})}{\partial p^{n+1,-}}, \tag{44b}$$

after division by the exponential term $e^{\gamma t^{n+1}}$. We see that the first step is implicit and the second step is explicit. The exponential term in (44a) needs some clarification. Using

$$1 - e^{\gamma(t^n - t^{n+1})} = 1 - e^{-\gamma \Delta t} \approx \gamma \Delta t, \tag{45}$$

shows that the discrete equation (44a) is an approximation to the damped equation

$$\dot{p} + \frac{\partial H}{\partial q} + \gamma p = 0. \tag{46}$$

This ensures that the modified total energy (41) will be preserved as will be demonstrated next.

5.1.2. Numerical results

Consider the Hamiltonian $H(p, q) = \frac{1}{2}p^2 + \frac{1}{2}q^2$. We compare three cases for the damped variational principle, viz. approximation (44a) and the more straightforward (forward and backward Euler) approximations for the damping term:

$$p^{n+1} = p^n - \Delta t \frac{\partial H(p^{n+1}, q^n)}{\partial q^n} - \Delta t \gamma p^n, \tag{47}$$

or

$$p^{n+1} = p^n - \Delta t \frac{\partial H(p^{n+1}, q^n)}{\partial q^n} - \Delta t \gamma p^{n+1}, \tag{48}$$

while the second equation (44b) in the system remains unchanged. We verify the absence of drift in a discrete version of the modified energy (41) at each time level t_n , $n = 0, \dots, N$,

$$H_{ex}(p^{n,-}, q^{n,+}, t^n) = \frac{1}{2} \left((p^{n,-})^2 + (q^{n,+})^2 + \gamma p^{n,-} q^{n,+} \right) e^{\gamma t^n} \tag{49}$$

for the different approximations. The results of the discrete modified energy are presented in Fig. 9 for the different approximations versus time. We see, that the modified energy for approximation (44a) oscillates around the initial state, while the other two approximations reveal a drift in energy. The latter was expected for the forward Euler approximation of the forcing term in (47). Nevertheless, the result is unexpected for the implicit scheme (48), where the approximation of the damping term is done analogously to the symplectic Euler scheme. Therefore our variational approach allows also the derivation of time integrators that result in a bounded fluctuation of special integrals.

5.2. Forced oscillator

A Hamiltonian system is studied that has a Lagrangian (1) with a forcing $f(p, q, t)$ added

$$\mathcal{L}(p, q) := \int_0^T \left(p \frac{dq}{dt} - H(p, q) - f(p, q, t) \right) dt. \quad (50)$$

We consider the simple case of a forced oscillator. The Hamiltonian is $H(p, q) = \frac{1}{2}p^2 + \frac{1}{2}q^2$ with forcing function $f(p, q, t) = -a\gamma tq$, where $a\gamma$ is the amplitude. The corresponding system reads

$$\frac{dq}{dt} = p \quad \text{and} \quad \frac{dp}{dt} = -q + a\gamma t. \quad (51)$$

This system is non-autonomous, but we can introduce a coordinate transformation to make it autonomous, as follows

$$q = Q + a\gamma t, \quad p = P. \quad (52)$$

The Lagrangian (50) for a forced harmonic oscillator is then reformulated as

$$\mathcal{L}(p, q) = \int_0^T \left(P \frac{dQ}{dt} - \left(\frac{1}{2}P^2 + \frac{1}{2}Q^2 - a\gamma P \right) \right) dt + \frac{1}{6}a^2\gamma^2 T^3. \quad (53)$$

An important quantity to monitor is the Hamiltonian in the new coordinates

$$\hat{H} = \frac{1}{2}P^2 + \frac{1}{2}Q^2 - a\gamma P, \quad (54)$$

which will be used to compute the order of accuracy of the forced scheme. The exact solution to the problem (51) is

$$q_{ex} = q(0) \cos(t) + (p(0) - a\gamma) \sin(t) + a\gamma t. \quad (55)$$

Next, we will consider the symplectic Störmer–Verlet scheme to compute the evolution of this forced system.

5.2.1. Forced symplectic Störmer–Verlet scheme

We consider the second order approximation with added forcing, and investigate the accuracy for different discretizations of the forcing term. We construct a Störmer–Verlet time stepping method adjoint to the one discussed in detail in §3.2. We take appropriate polynomial approximations (15), the mixed quadrature rule (16) and $\alpha = 0$. Then we obtain a discrete approximation of the Lagrangian (50) formulated as follows

$$\begin{aligned} \mathcal{L}^\tau(p^\tau, q^\tau) = & \sum_{n=0}^{N-1} \left(p^{n+1/2} (q^{n+1,-} - q^{n,+}) \right. \\ & \left. - \frac{\Delta t}{2} \left(H(p^{n+1/2}, q^{n,+}) + H(p^{n+1/2}, q^{n+1,-}) \right) \right) \\ & \left. - \frac{\Delta t}{2} \left(f(p^{n+1/2}, q^{n,+}, t^*) + f(p^{n+1/2}, q^{n+1,-}, t^{**}) \right) \right) \\ & - \sum_{n=-1}^{N-1} (q^{n+1,-} - q^{n+1,+}) p^{n+1,+}. \end{aligned} \quad (56)$$

Computing the variations, we obtain the following system of equations

$$\delta p^{n,+} : q^{n+1,+} = q^{n+1,-}, \quad (57a)$$

$$\delta q^{n,+} : p^{n+1/2} = p^{n,+} - \frac{\Delta t}{2} \frac{\partial H(p^{n+1/2}, q^{n,+})}{\partial q^{n,+}} - \frac{\Delta t}{2} \frac{\partial f(p^{n+1/2}, q^{n,+}, t^*)}{\partial q^{n,+}}, \quad (57b)$$

$$\begin{aligned} \delta p^{n+1/2} : q^{n+1,-} = & q^{n,+} + \frac{\Delta t}{2} \left(\frac{\partial H(p^{n+1/2}, q^{n,+})}{\partial p^{n+1/2}} + \frac{\partial H(p^{n+1/2}, q^{n+1,-})}{\partial p^{n+1/2}} \right), \\ & + \frac{\Delta t}{2} \left(\frac{\partial f(p^{n+1/2}, q^{n,+}, t^*)}{\partial p^{n+1/2}} + \frac{\partial f(p^{n+1/2}, q^{n+1,-}, t^{**})}{\partial p^{n+1/2}} \right) \end{aligned} \quad (57c)$$

$$\delta q^{n+1,-} : p^{n+1,+} = p^{n+1/2} - \frac{\Delta t}{2} \frac{\partial H(p^{n+1/2}, q^{n+1,-})}{\partial q^{n+1,-}} - \frac{\Delta t}{2} \frac{\partial f(p^{n+1/2}, q^{n+1,-}, t^{**})}{\partial q^{n+1,-}}, \quad (57d)$$

Table 2

Convergence in the L^∞ -norm of the error in q for a forced harmonic oscillator. We denote (57) with the forcing term integral approximated as (58) by SV1, and (57) with the forcing term integral as (59) by SV2.

Step	SV1		SV2	
	L_{err}^∞	order	L_{err}^∞	order
Δt	2.2291E-1	-	2.2041E-1	-
$\Delta t/2$	6.2108E-2	1.8436	6.1503E-2	1.8414
$\Delta t/4$	1.5590E-2	1.9942	1.5466E-2	1.9915
$\Delta t/8$	3.8804E-3	2.0063	3.8516E-3	2.0056
$\Delta t/16$	9.6874E-4	2.0020	9.6168E-4	2.0018
$\Delta t/32$	2.4210E-4	2.0005	2.4034E-4	2.0005
$\Delta t/64$	6.0518E-5	2.0001	6.0080E-5	2.0001

Table 3

Convergence in the L^2 -norm of the error in q for a forced harmonic oscillator. For details, see the caption of Table 2.

Step	SV1		SV2	
	L_{err}^2	order	L_{err}^2	order
Δt	6.8361E-1	-	6.7380E-1	-
$\Delta t/2$	1.7151E-1	1.9949	1.6961E-1	1.9901
$\Delta t/4$	4.2441E-2	2.0147	4.2012E-2	2.0134
$\Delta t/8$	1.0576E-2	2.0047	1.0471E-2	2.0043
$\Delta t/16$	2.6417E-3	2.0012	2.6158E-3	2.0011
$\Delta t/32$	6.6029E-4	2.0003	6.5381E-4	2.0003
$\Delta t/64$	1.6506E-4	2.0001	1.6344E-4	2.0001

Table 4

Convergence of the extended energy error (60c) for a forced harmonic oscillator. For details, see the caption of Table 2.

Step	SV1		SV2	
	$\Delta \hat{H}_{err}$	order	$\Delta \hat{H}_{err}$	order
Δt	2.7500E-3	-	3.0625E-3	-
$\Delta t/2$	7.1553E-4	1.9423	8.0497E-4	1.9277
$\Delta t/4$	1.7416E-4	2.0386	1.9731E-4	2.0285
$\Delta t/8$	4.3256E-5	2.0094	4.9234E-5	2.0027
$\Delta t/16$	1.0797E-5	2.0023	1.2296E-5	2.0015
$\Delta t/32$	2.6981E-6	2.0006	3.0731E-6	2.0004
$\Delta t/64$	6.7446E-7	2.0001	7.6824E-7	2.0001

where we decide on the choice of the time levels t^* and t^{**} later. Convergence tests will be performed to compare different forcing term approximations. We use the following approximations of the integral on the forcing term in (57)

$$\int_{t_n}^{t_{n+1}} f(p^\tau, q^\tau, t) dt = \frac{\Delta t}{2} \left(f(p^{n+1/2}, q^{n,+}, t^n) + f(p^{n+1/2}, q^{n+1,-}, t^{n+1}) \right) \text{ or} \tag{58}$$

$$= \frac{\Delta t}{2} \left(f(p^{n+1/2}, q^{n,+}, t^{n+1/2}) + f(p^{n+1/2}, q^{n+1,-}, t^{n+1/2}) \right). \tag{59}$$

The convergence tests are based on the L^∞ -norm, see Table 2, and the L^2 -norm, see Table 3. Estimates of the extended energy error (54) is given in Table 4. The exact solution q_{ex} in (55) is used.

The set up of the numerical test is as follows. We start with $\Delta t = 1$, the number of time steps is $N = 40$. The final time, where we compare the results, is $T = 40$. The amplitude of the forcing is $a = 0.1$ with $\gamma = 0.1$. The initial coordinate $q_0 = 0.1$ and the initial momentum $p_0 = -0.1$. The errors are defined as

$$L_{err}^\infty = \max_{1 \leq n \leq N} |q^n - q_{ex}(t^n)|, \tag{60a}$$

$$L_{err}^2 = \sqrt{\sum_{n=1}^N \int_{t^{n-1}}^{t^n} (q^\tau - q_{ex}(t))^2 dt}, \text{ and} \tag{60b}$$

$$\Delta \hat{H}_{err} = \max_{1 \leq n \leq N} (\hat{H}(p^n, q^n, t^n)) - \min_{1 \leq n \leq N} (\hat{H}(p^n, q^n, t^n)), \tag{60c}$$

where q^τ is an approximation of q in the time interval (t^{n-1}, t^n) . For the second order approximation considered here, we have q^τ defined in (15).

These schemes are all second order accurate and the extended energy \hat{H} is bounded and reveals no drift in time. One of these approaches was successfully used for the variational water wave problem with a wave maker in [9].

6. Nonlinear potential flow water waves

We investigate the performance of the third order symplectic time integrator (23) to compute nonlinear potential flow water waves in a water basin. The dynamics of the water waves can be embedded in Miles’ variational principle [21]. For a wave basin with solid boundaries this variational principle is

$$0 = \delta \mathcal{L}(\phi, \eta, \phi_s) := \delta \int_0^T \left(\int_0^L \left(\phi_s \frac{\partial \eta}{\partial t} - \frac{1}{2} g(\eta^2 - b^2) \right) dx - \int_0^L \int_{-b(x)}^{\eta(x,t)} \frac{1}{2} |\nabla \phi|^2 dz dx \right) dt. \tag{61}$$

The domain $\Omega = \{0 < x < L, -b(x) < z < \eta(x, t)\} \subset \mathbb{R}^2$ is time dependent due to the movement of the free surface boundary $S_F : z = \eta(x, t)$. The bottom is fixed $S_B : z = -b(x)$, and also the solid walls to the left and right of the basin: $S_L : x = 0, x = L$ are fixed. The velocity potential is denoted by $\phi(x, z, t)$, and $\phi_s(x, t) = \phi(x, z = \eta, t)$ is the velocity potential at the free surface; ∇ is the gradient operator. The total energy or Hamiltonian of the system is the sum of potential plus kinetic energies

$$H(\phi, \eta, \phi_s) := \int_0^L \frac{1}{2} g(\eta^2 - b^2) dx + \int_0^L \int_{-b(x)}^{\eta(x,t)} \frac{1}{2} |\nabla \phi|^2 dz dx. \tag{62}$$

By taking the variational derivatives with respect to ϕ, η, ϕ_s and the velocity potential at the fixed boundaries $\phi(0, z, t), \phi(L, z, t), \phi(x, -b, t)$, in (61) we obtain the potential flow equation with nonlinear boundary conditions [18,21,9].

When we substitute finite element approximations at the free surface $\eta \approx \eta_h(x, t) = \eta_l(t)\varphi_l(x), \phi_s \approx \phi_{sh}(x, t) = \phi_k(t)\varphi_k(x)$ and $\phi \approx \phi_h(x, z, t) = \phi_i(t)\tilde{\varphi}_i(x, z)$ into (61) the space discrete variational principle takes the form

$$0 = \delta \int_0^T L(\phi_{i'}, \phi_k, \eta_l) dt = \delta \int_0^T \left(M_{kl} \phi_k \frac{d\eta_l}{dt} - \frac{1}{2} g M_{kl} \eta_k \eta_l - \frac{1}{2} A_{ij} \phi_i \phi_j \right) dt, \tag{63}$$

with M_{kl} the symmetric mass matrix and A_{ij} the symmetric matrix associated with the kinetic energy and Laplace operator, given standard Lagrange basis functions $\varphi_l(x)$ and $\tilde{\varphi}_i(x, z)$. Summation over repeated indices is used. Indices k and l concern free surface nodes and degrees of freedom, indices i and j concern all nodes and degrees of freedom, while indices i' and j' concern the interior nodes and degrees of freedom (so excluding the free surface ones). For detailed definitions we refer the reader to [8,9].

The basis functions in the interior remain time dependent as they follow the free surface movement. The Hamiltonian (62) is approximated as

$$H(\boldsymbol{\phi}, \boldsymbol{\eta}) = \frac{1}{2} g M_{kl} \eta_k \eta_l + \frac{1}{2} A_{ij}(\boldsymbol{\eta}) \phi_i \phi_j, \tag{64}$$

where the boldface variables denote the vectors of unknown coefficients.

Further, as in [9], we need to approximate the variables in time. We choose within each time interval $t \in (t^n, t^{n+1})$, with $t^{n+1} = t^n + \Delta t$, a quadratic expansion in time analogous to the expansion (17). Then the free surface η and potential ϕ are approximated as:

$$\eta_l = \frac{(t^n + t^{n+1} - 2t)(t^{n+1} - t)}{\Delta t^2} \eta_l^{n,+} + \frac{4(t - t^n)(t^{n+1} - t)}{\Delta t^2} \eta_l^{n+1/2} - \frac{(t^n + t^{n+1} - 2t)(t - t^n)}{\Delta t^2} \eta_l^{n+1,-}, \tag{65a}$$

$$\phi_i = \frac{(t^n + t^{n+1} - 2t)(t^{n+1} - t)}{\Delta t^2} \phi_i^{n,+} + \frac{4(t - t^n)(t^{n+1} - t)}{\Delta t^2} \phi_i^{n+1/2} - \frac{(t^n + t^{n+1} - 2t)(t - t^n)}{\Delta t^2} \phi_i^{n+1,-}. \tag{65b}$$

Using approximations (65) we obtain an approximation of the continuous variational principle (61) similar to (19), resulting in the discrete minimization problem

$$\begin{aligned} 0 &= \delta \sum_{n=0}^{N-1} L(\phi_i^{n,+}, \eta_l^{n,+}, \phi_i^{n+1/2}, \eta_l^{n+1/2}, \phi_i^{n+1,-}, \eta_l^{n+1,-}) \\ &= \delta \sum_{n=0}^{N-1} M_{kl} \left(\frac{1}{6} \phi_k^{n,+} (-3\eta_l^{n,+} + 4\eta_l^{n+1/2} - \eta_l^{n+1,-}) \right) \end{aligned}$$

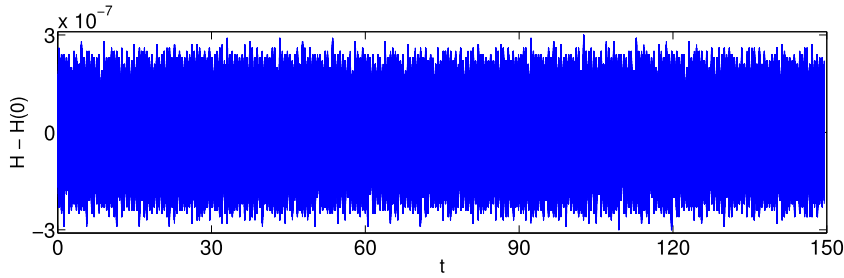


Fig. 10. Error in the energy for standing waves in a basin after one hundred time periods. A triangular tessellation is used with $N_x = 81$, $N_z = 5$ and time step $\Delta t = 0.00625$. The precision to solve the implicit subsystem is $\epsilon = 10^{-12}$.

$$\begin{aligned}
 & + \frac{2}{3} \phi_k^{n+1/2} (-\eta_l^{n,+} + \eta_l^{n+1,-}) + \frac{1}{6} \phi_k^{n+1,-} (\eta_l^{n,+} - 4\eta_l^{n+1/2} + 3\eta_l^{n+1,-}) \\
 & - \frac{\Delta t}{6} \left(H(\phi_i^{n,+}, \eta_l^{n,+}) + 4H(\phi_i^{n+1/2}, \eta_l^{n+1/2}) + H(\phi_i^{n+1,-}, \eta_l^{n+1,-}) \right) \\
 & - \delta \sum_{n=-1}^{N-1} \frac{1}{2} M_{kl} (\eta_l^{n+1,-} - \eta_l^{n+1,+}) (\phi_k^{n+1,-} + \phi_k^{n+1,+}).
 \end{aligned} \tag{66}$$

Variation of (66) with respect to the independent variables $\phi_k^{n,+}$, $\eta_l^{n,+}$, $\phi_k^{n+1/2}$, $\phi_{j'}^{n+1/2}$, $\eta_l^{n+1/2}$, $\phi_k^{n+1,-}$, $\phi_{j'}^{n+1,-}$, $\eta_l^{n+1,-}$ gives the following variational discretization

$$\begin{cases}
 M_{kl} \eta_l^{n+1/2} = \frac{3}{4} M_{kl} \eta_l^{n,-} + \frac{1}{4} M_{kl} \eta_l^{n,+} + \frac{\Delta t}{4} \left(\frac{\partial H(\phi_i^{n,+}, \eta_l^{n,+})}{\partial \phi_k^{n,+}} + \frac{\partial H(\phi_i^{n+1/2}, \eta_l^{n+1/2})}{\partial \phi_k^{n+1/2}} \right), \\
 M_{kl} \phi_k^{n+1/2} = \frac{3}{4} M_{kl} \phi_k^{n,-} + \frac{1}{4} M_{kl} \phi_k^{n,+} - \frac{\Delta t}{4} \left(\frac{\partial H(\phi_i^{n,+}, \eta_l^{n,+})}{\partial \eta_l^{n,+}} + \frac{\partial H(\phi_i^{n+1/2}, \eta_l^{n+1/2})}{\partial \eta_l^{n+1/2}} \right), \\
 A_{i'j'}(\eta^{n+1/2}) \phi_{i'}^{n+1/2} = -A_{kj'}(\eta^{n+1/2}) \phi_k^{n+1/2}, \\
 M_{kl} \eta_l^{n+1,-} = M_{kl} \eta_l^{n,+} + \Delta t \frac{\partial H(\phi_i^{n+1/2}, \eta_l^{n+1/2})}{\partial \phi_k^{n+1/2}}, \\
 M_{kl} \phi_k^{n+1,-} = M_{kl} \phi_k^{n,+} - \Delta t \frac{\partial H(\phi_i^{n+1/2}, \eta_l^{n+1/2})}{\partial \eta_l^{n+1/2}}, \\
 A_{i'j'}(\eta^{n+1,-}) \phi_{i'}^{n+1,-} = -A_{kj'}(\eta^{n+1,-}) \phi_k^{n+1,-}, \\
 M_{kl} \eta_l^{n+1,+} = \frac{4}{3} M_{kl} \eta_l^{n+1/2} - \frac{1}{3} M_{kl} \eta_l^{n,+} + \frac{\Delta t}{3} \frac{\partial H(\phi_i^{n+1,-}, \eta_l^{n+1,-})}{\partial \phi_k^{n+1,-}}, \\
 M_{kl} \phi_k^{n+1,+} = \frac{4}{3} M_{kl} \phi_k^{n+1/2} - \frac{1}{3} M_{kl} \phi_k^{n,+} - \frac{\Delta t}{3} \frac{\partial H(\phi_i^{n+1,-}, \eta_l^{n+1,-})}{\partial \eta_l^{n+1,-}}, \\
 A_{i'j'}(\eta^{n+1,+}) \phi_{i'}^{n+1,+} = -A_{kj'}(\eta^{n+1,+}) \phi_k^{n+1,+}.
 \end{cases} \tag{67}$$

As verification test, we consider standing waves in a rectangular basin with a unit depth $H = 1$ and the basin length $L = 10$. A linear solution is used to set the initial condition at $t = 0$

$$\eta(x, t) = \frac{A\omega}{g} \cos(kx) \sin(\omega t) \cosh(kH); \quad \phi(x, z, t) = A \cos(kx) \cos(\omega t) \cosh(kz), \tag{68}$$

with amplitude $A = 0.075$, wave number $k = 2\pi N_w/L$, with integer $N_w = 3$, and the dispersion relation $\omega^2 = gk \tanh(kH)$. The waves computed with the variational discretization (67) show no decay in discrete energy over one hundred periods of time, as can be seen in Fig. 10. The error in the discrete energy is used to compute the order of accuracy. As we can see in Table 5, the scheme is third order accurate in time.

The time integration method (67) poses a conceptual advantage compared to the second order Störmer–Verlet scheme, presented in this section, see also [9]. The Störmer–Verlet scheme requires a trapezoidal-midpoint quadrature rule, which makes it more difficult to determine the times at which the interior potential has to be evaluated, because the discrete Neumann operator (the inverse of $A_{i',j'}$) has to be applied first. The interior velocity potential depends on the free surface elevation and the free surface velocity potential. It results in an unsymmetrical approximation of the variables, which is not optimal. The surface elevation is approximated in time via $\eta_s^{n,+}$ and $\eta_s^{n+1,-}$, while the free surface potential is approximated via $\phi_s^{n,+}$ and $\phi_s^{n+1/2}$. The resulting numerical discretization, which is discussed in [9], provided excellent results,

Table 5

Convergence of the energy error for standing waves in a square basin using the third order symplectic time integrator (67). See Fig. 10 for the parameter values used. The results are compared after ten time periods.

Step	ΔH -error	order
Δt	2.9372E-4	–
$\Delta t/2$	3.66132E-5	3.0040
$\Delta t/4$	4.5574E-6	3.0060
$\Delta t/8$	5.6923E-7	3.0011
$\Delta t/16$	7.1200E-8	2.9991
$\Delta t/32$	8.8996E-9	3.0001
$\Delta t/64$	1.1124E-9	3.0000

but it also required a lot of additional analysis. In contrast, the method (67) is symmetrical and therefore there is no question of how to compute the velocity potential in the interior. Moreover, method (67) solves one implicit system with three equations, then six explicit steps and gives third order accuracy, while the Störmer–Verlet scheme solves an implicit system for ϕ_I, ϕ_S first, then an implicit system for η_S, ϕ_I and one explicit step for ϕ_S . Therefore the second order scheme requires the solution of two uncoupled implicit systems of equations versus one coupled set of equations for the third order scheme.

7. Conclusions

We have constructed novel symplectic time integrators using a variational approach. The time integration method is based on a discontinuous Galerkin discretization in time, using a novel numerical flux, which connects the adjacent time slabs. We first demonstrated how several well-known time integrators, such as the symplectic Euler and Störmer–Verlet time integrators, can be derived using this variational approach. Subsequently, a new symplectic time integrator was derived third order accurate in time. The third order time integrator was shown to have excellent dispersion properties and was also successfully applied to compute nonlinear water waves in a basin. Finally, the variational approach to derive time stepping schemes was also developed and tested for non-autonomous Hamiltonian systems, such as forced and damped oscillators as well as driven water wave problems (see also [3]).

Acknowledgements

We acknowledge financial support of the Technology Foundation STW and The Netherlands Organization for Scientific Research (NWO) for the projects “Complex wave current interactions in a numerical wave tank”, STW grant no. 08130, and “Compatible Mathematical Models for Coastal Hydrodynamics”, NWO grant no. 613.000.803, as well as Bokhove’s EPSRC grant no. EP/L025388/1 “FastFem: Behaviour of Fast ships in waves”.

Appendix A. Continuum harmonic oscillator

In this section we will show the essential steps in the analysis of the harmonic oscillator following work in [2]. The dynamics of a harmonic oscillator is embedded in the functional

$$\mathcal{L}(p, q) := \int_0^T \left(p \frac{dq}{dt} - H(p, q) \right) dt, \quad (\text{A.1})$$

with $p(t)$ the momentum, $q(t)$ the coordinate and $H(p, q)$ the energy (or Hamiltonian) of the oscillator, which is defined as

$$H(p, q) := \frac{1}{2} p^2 + \frac{1}{2} \omega^2 q^2, \quad (\text{A.2})$$

with the frequency ω . The variational derivative of this Hamiltonian is

$$\delta H(p, q) := \frac{\partial H}{\partial p} \delta p + \frac{\partial H}{\partial q} \delta q = p \delta p + \omega^2 q \delta q. \quad (\text{A.3})$$

From the variational principle $\delta \mathcal{L}(p, q) = 0$ with end-point conditions $\delta q(0) = 0, \delta q(T) = 0$, the dynamics of the harmonic oscillator emerges:

$$\begin{pmatrix} p \\ q \end{pmatrix}_t = \begin{pmatrix} 0 & -\omega^2 \\ 1 & 0 \end{pmatrix} \begin{pmatrix} p \\ q \end{pmatrix} = A \begin{pmatrix} p \\ q \end{pmatrix}, \quad (\text{A.4})$$

with initial conditions $p(t = 0) = p_0$ and $q(t = 0) = q_0$. Subscript t refers to differentiation in time. The characteristic polynomial for system matrix A is

$$\lambda^2 + \omega^2 = 0 \tag{A.5}$$

with eigenvalues $\lambda = \pm i\omega$.

Following, e.g. [15], we can find the dispersion relation by taking a Fourier mode

$$\begin{pmatrix} p \\ q \end{pmatrix} = \begin{pmatrix} ae^{-i\hat{\omega}t} \\ be^{-i\hat{\omega}t} \end{pmatrix}. \tag{A.6}$$

Solving it, we arrive at

$$\hat{\omega} = \omega, \quad a = -i\omega b \quad \text{or} \quad \hat{\omega} = -\omega, \quad a = i\omega b. \tag{A.7}$$

Finally, the exact solution of this system used in convergence tests is

$$\begin{pmatrix} p \\ q \end{pmatrix} = \begin{pmatrix} \cos(\omega t) & -\omega \sin(\omega t) \\ \frac{1}{\omega} \sin(\omega t) & \cos(\omega t) \end{pmatrix} \begin{pmatrix} p_0 \\ q_0 \end{pmatrix}. \tag{A.8}$$

Appendix B. Störmer–Verlet scheme

In this section we provide the details of the analysis of the scheme given by (14) and introduced in Section 3.2. We demonstrate that the scheme coincides with the Störmer–Verlet time stepping scheme.

In the system of equations (14) we have three variables from the time slab (t^{n-1}, t^n) : $q^{n-1,+}$, $q^{n-1/2}$, $p^{n,-}$; four variables from the time slab (t^n, t^{n+1}) : $p^{n,+}$, $q^{n,+}$, $q^{n+1/2}$, $p^{n+1,-}$, and two variables from the time slab (t^{n+1}, t^{n+2}) : $p^{n+1,+}$, $q^{n+1,+}$. One can notice that variables $q^{n-1/2}$, $q^{n-1,+}$ appear only in combination. To make the system solvable, we reformulate (14) with the variables $[[q]]|_{t_{n+1}}$, $q^{n+1/2}$ and $[[p]]|_{t_{n+1}}$ and $p^{n+1,-}$ as unknowns:

$$\delta q^{n,+} : \beta [[p]]|_{t_{n+1}} = \alpha [[p]]|_{t_n}, \tag{B.1a}$$

$$\delta p^{n,+} : q^{n+1/2} = q^{n,+} + \beta [[q]]|_{t_n} + \frac{\Delta t}{2} \frac{\partial H(p^{n,+}, q^{n+1/2})}{\partial p^{n,+}}, \tag{B.1b}$$

$$\delta q^{n+1/2} : p^{n+1,-} = p^{n,+} + 2\beta [[p]]|_{t_{n+1}} - \frac{\Delta t}{2} \left(\frac{\partial H(p^{n,+}, q^{n+1/2})}{\partial q^{n+1/2}} + \frac{\partial H(p^{n+1,-}, q^{n+1/2})}{\partial q^{n+1/2}} \right), \tag{B.1c}$$

$$\delta p^{n+1,-} : \alpha [[q]]|_{t_{n+1}} = q^{n+1/2} - q^{n,+} - \frac{\Delta t}{2} \frac{\partial H(p^{n+1,-}, q^{n+1/2})}{\partial p^{n+1,-}}. \tag{B.1d}$$

In addition, we have the relations: $q^{n+1,+} = q^{n+1,-} - [[q]]|_{t_{n+1}} = 2q^{n+1/2} - q^{n,+} - [[q]]|_{t_{n+1}}$, and $p^{n+1,+} = p^{n+1,-} - [[p]]|_{t_{n+1}}$. Hence, there are enough equations to close the system.

B.1. Linear stability

To study the linear stability of the system (B.1), we take $H = \frac{1}{2}p^2 + \frac{1}{2}\omega^2q^2$. For this Hamiltonian, system (B.1) is rewritten in matrix form as

$$\begin{pmatrix} [[p]]|_{t_{n+1}} \\ p^{n+1,+} \\ [[q]]|_{t_{n+1}} \\ q^{n+1,+} \end{pmatrix} \equiv A^n \begin{pmatrix} [[p]]|_{t^n} \\ p^{n,+} \\ [[q]]|_{t^n} \\ q^{n,+} \end{pmatrix} = \begin{pmatrix} \frac{\alpha}{\beta} & \vdots & 0 & \vdots & 0 & \vdots & 0 \\ 2\alpha - \frac{\alpha}{\beta} & \vdots & 1 - \frac{\Delta t^2 \omega^2}{2} & \vdots & -\Delta t \omega^2 \beta & \vdots & -\Delta t \omega^2 \\ -\Delta t & \vdots & \frac{\Delta t^3 \omega^2}{4\alpha} & \vdots & \frac{\beta}{\alpha} \left(1 + \frac{\Delta t^2 \omega^2}{2} \right) & \vdots & \frac{\Delta t^2 \omega^2}{2\alpha} \\ \Delta t & \vdots & \Delta t - \frac{\Delta t^3 \omega^2}{4\alpha} & \vdots & 2\beta - \frac{\beta}{\alpha} - \frac{\Delta t^2 \omega^2 \beta}{2\alpha} & \vdots & 1 - \frac{\Delta t^2 \omega^2}{2\alpha} \end{pmatrix} \begin{pmatrix} [[p]]|_{t^n} \\ p^{n,+} \\ [[q]]|_{t^n} \\ q^{n,+} \end{pmatrix}. \tag{B.2}$$

The characteristic polynomial of matrix A^n has the form

$$\left(\frac{\alpha}{\beta} - \lambda\right) \left(\frac{\beta}{\alpha} - \lambda\right) (\lambda^2 + (\omega^2 (\Delta t)^2 - 2)\lambda + 1) = 0, \tag{B.3}$$

from which we can see that the necessary condition to satisfy the linear stability requirement $|\lambda| \leq 1$ is to take $\alpha = \beta = 0.5$. Nevertheless, this restriction can be alleviated by taking $[[p]]|_{t_n} \equiv 0$. In this case the first row of the transformation matrix A^n in (B.2), will be removed and the characteristic polynomial (B.3) reduces to

$$\left(\frac{\beta}{\alpha} - \lambda\right)(\lambda^2 + (\omega^2(\Delta t)^2 - 2)\lambda + 1) = 0, \quad (\text{B.4})$$

which gives two linear stability requirements:

$$\alpha \geq 0.5 \quad \text{and} \quad |\omega\Delta t| \leq 2. \quad (\text{B.5})$$

Therefore, if $[[p]]|_{t_n} \equiv 0$, a range of weights $\alpha \in [0.5, 1]$ leads to a stable system under the usual Störmer–Verlet stability condition.

B.2. Derivation of classical Störmer–Verlet scheme

Considering the above mentioned requirement $\alpha \in [0.5, 1]$, $[[p]]|_{t_n} \equiv 0$, we can recover the well-known form of the unforced symplectic Störmer–Verlet scheme. First, we rewrite (B.1) as

$$\delta q^{n,+} : p^{n,+} = p^{n,-}, \quad (\text{B.6a})$$

$$\delta p^{n,+} : q^{n+1/2} = \beta q^{n,-} + \alpha q^{n,+} + \frac{\Delta t}{2} \frac{\partial H(p^{n,+}, q^{n+1/2})}{\partial p^{n,+}}, \quad (\text{B.6b})$$

$$\delta q^{n+1/2} : p^{n+1,-} = p^{n,+} - \frac{\Delta t}{2} \left(\frac{\partial H(p^{n,+}, q^{n+1/2})}{\partial q^{n+1/2}} + \frac{\partial H(p^{n+1,-}, q^{n+1/2})}{\partial q^{n+1/2}} \right), \quad (\text{B.6c})$$

$$\delta p^{n+1,-} : \beta q^{n+1,-} + \alpha q^{n+1,+} = q^{n+1/2} + \frac{\Delta t}{2} \frac{\partial H(p^{n+1,-}, q^{n+1/2})}{\partial p^{n+1,-}}. \quad (\text{B.6d})$$

We see from (B.6a), that we can denote $p^n := p^{n,+} = p^{n,-}$. Also, one can introduce a variable $q^n := \beta q^{n,-} + \alpha q^{n,+}$, and recover the known form of the system, where the first and second steps are implicit and the third step is explicit

$$q^{n+1/2} = q^n + \frac{\Delta t}{2} \frac{\partial H(p^n, q^{n+1/2})}{\partial p^n}, \quad (\text{B.7a})$$

$$p^{n+1} = p^n - \frac{\Delta t}{2} \left(\frac{\partial H(p^n, q^{n+1/2})}{\partial q^{n+1/2}} + \frac{\partial H(p^{n+1}, q^{n+1/2})}{\partial q^{n+1/2}} \right), \quad (\text{B.7b})$$

$$q^{n+1} = q^{n+1/2} + \frac{\Delta t}{2} \frac{\partial H(p^{n+1}, q^{n+1/2})}{\partial p^{n+1}}. \quad (\text{B.7c})$$

The resulting scheme is the symplectic Störmer–Verlet integrator [12]. The characteristic polynomial for the transformation matrix of this scheme has the form

$$\lambda^2 + (\omega^2(\Delta t)^2 - 2)\lambda + 1 = 0. \quad (\text{B.8})$$

The eigenvalues λ therefore satisfy the condition $|\lambda| \leq 1$ if $|\Delta t\omega| \leq 2$, which is the well-known stability condition for the Störmer–Verlet scheme. The dispersion relation, as discussed, for example, in [2], has the form

$$a = -i\omega b \sqrt{1 - \frac{\omega^2 \Delta t^2}{4}}, \quad \hat{\omega} = \frac{\arccos(1 - \frac{\omega^2(\Delta t)^2}{2})}{\Delta t}. \quad (\text{B.9})$$

References

- [1] V.I. Arnold, *Mathematical Methods of Classical Mechanics*, Grad. Texts Math., vol. 60, Springer, 1989. Originally published by Nauka, Moscow, 1974, 2nd ed., vol. XVI, 1989, 519 pp.
- [2] J. Bajars, *Geometric integration and thermostat methods for Hamiltonian systems*, PhD thesis, University of Amsterdam (UvA), Amsterdam, December 2012.
- [3] O. Bokhove, A. Kalogirou, Variational water wave modelling: from continuum to experiment, in: T. Bridges, M. Groves, D. Nicholls (Eds.), *Lectures on the Theory of Water Waves*, in: LMS Lecture Note Series, Cambridge University Press, United Kingdom, 2016, pp. 226–260.
- [4] C. Dal Maso, P.G. LeFloch, F. Murat, Definition and weak stability of nonconservative products, *J. Math. Pures Appl.* 74 (1995) 483–548.
- [5] M. Delfour, W. Hager, F. Trochu, Discontinuous Galerkin methods for ordinary differential equations, *Math. Comput.* 36 (154) (1981) 455–473.
- [6] M.C. Delfour, F. Dubeau, Discontinuous polynomial approximations in the theory of one-step, hybrid and multistep methods for nonlinear ordinary differential equations, *Math. Comput.* 47 (175) (1986) 169–189.
- [7] D. Estep, D. French, Global error control for the continuous Galerkin finite element method for ordinary differential equations, *Modél. Math. Anal. Numér.* 28 (1994) 815–852.
- [8] E. Gagarina, *Variational approaches to water wave simulations*, PhD thesis, Univ. of Twente, Enschede, October 2014.
- [9] E. Gagarina, V.R. Ambati, J.J.W. van der Vegt, O. Bokhove, Variational space–time (dis)continuous Galerkin method for nonlinear free surface water waves, *J. Comput. Phys.* 275 (0) (2014) 459–483.
- [10] S. Zhao, G.W. Wei, A unified discontinuous Galerkin framework for time integration, *Math. Methods Appl. Sci.* 37 (2014) 1042–1071.

- [11] M. Gross, Conserving time integrators for nonlinear elastodynamics, PhD thesis, Department of Mechanical Engineering, University of Kaiserslautern, 2004.
- [12] E. Hairer, C. Lubich, G. Wanner, Geometric Numerical Integration, 2nd ed., Springer Ser. Comput. Math., Springer, Berlin, 2006.
- [13] J. Hall, M. Leok, Lie Group Spectral Variational Integrators, *Found. Comput. Math.*, 2015, pp. 1–59.
- [14] J. Hennig, C.E. Schmittner, Experimental variation of focusing wave groups for the investigation of their predictability, in: *Materials Technology*, vol. 6; C.C. Mei, Symposium on Wave Mechanics and Hydrodynamics; Offshore Measurement and Data Interpretation, Proc. ASME 2009 28th Int. Conf. on Ocean, Offshore and Arctic Engineering, Honolulu, Hawaii, USA, June 2009, p. 11.
- [15] E. Kalnay, Atmospheric Modeling, Data Assimilation and Predictability, Cambridge University Press, 2003.
- [16] B. Leimkuhler, S. Reich, Simulating Hamiltonian Dynamics, vol. 14, Cambridge University Press, 2004.
- [17] M. Leok, T. Shingel, General techniques for constructing variational integrators, *Front. Math. China* 7 (2) (2012) 273–303.
- [18] J.C. Luke, A variational principle for a fluid with a free surface, *J. Fluid Mech.* 27 (2) (1967) 395–397.
- [19] J.E. Marsden, T.S. Ratiu, Introduction to Mechanics and Symmetry: A Basic Exposition of Classical Mechanical Systems, vol. 17, Springer, 1999.
- [20] J.E. Marsden, M. West, Discrete mechanics and variational integrators, *Acta Numer.* 2001 10 (2001) 357–514.
- [21] J.W. Miles, On Hamilton's principle for surface waves, *J. Fluid Mech.* 83 (1977) 153–158.
- [22] S. Ober-Blöbaum, N. Saake, Construction and analysis of higher order Galerkin variational integrators, *Adv. Comput. Math.* XX (2014) 1–32.
- [23] P.J. Olver, Applications of Lie Groups to Differential Equations, 2nd ed., Grad. Texts Math., vol. 107, Springer-Verlag, 1993.
- [24] S. Rhebergen, Discontinuous Galerkin finite element methods for (non)conservative partial differential equations, PhD thesis, Univ. of Twente, Enschede, February 2010.
- [25] S. Rhebergen, O. Bokhove, J.J.W. van der Vegt, Discontinuous Galerkin finite element methods for hyperbolic nonconservative partial differential equations, *J. Comput. Phys.* 227 (3) (2008) 1887–1922.
- [26] Y. Suris, Hamiltonian methods of Runge–Kutta type and their variational interpretation, *Math. Model.* 2 (4) (1990) 78–87.
- [27] A.R. Thornton, A.J. van der Horn, E. Gagarina, W. Zweers, D. van der Meer, O. Bokhove, Hele–Shaw beach creation by breaking waves: a mathematics-inspired experiment, *Environ. Fluid Mech.* (2014) 1–23.
- [28] A.I. Vol'pert, The spaces BV and quasilinear equations, *Math. USSR Sb.* 2 (2) (1967) 225–267.
- [29] V.E. Zakharov, Stability of periodic waves of finite amplitude on the surface of a deep fluid, *J. Appl. Mech. Tech. Phys.* 9 (2) (1968) 190–194.